

## Can gas hydrate structures be described using classical simulations?

Maria M. Conde,<sup>1</sup> Carlos Vega,<sup>1,a)</sup> Carl McBride,<sup>1</sup> Eva G. Noya,<sup>2</sup> Rafael Ramírez,<sup>3</sup> and Luis M. Sesé<sup>4</sup>

<sup>1</sup>Dept. Química-Física I, Facultad de Ciencias Químicas, Universidad Complutense de Madrid, 28040 Madrid, Spain

<sup>2</sup>Instituto de Química Física Rocasolano, Consejo Superior de Investigaciones Científicas (CSIC), Calle Serrano 119, 28006 Madrid, Spain

<sup>3</sup>Instituto de Ciencia de Materiales, CSIC, Campus de Cantoblanco, 28049 Madrid, Spain

<sup>4</sup>Dept. Ciencias y Técnicas Fisicoquímicas, Facultad de Ciencias, UNED, Paseo Senda del Rey 9, 28040 Madrid, Spain

(Received 2 December 2009; accepted 13 February 2010; published online 15 March 2010)

Quantum path-integral simulations of the hydrate solid structures have been performed using the recently proposed TIP4PQ/2005 model. By also performing classical simulations using this model, the impact of the nuclear quantum effects on the hydrates is highlighted; nuclear quantum effects significantly modify the structure, densities, and energies of the hydrates, leading to the conclusion that nuclear quantum effects are important not only when studying the solid phases of water but also when studying the hydrates. To analyze the validity of a classical description of hydrates, a comparison of the results of the TIP4P/2005 model (optimized for classical simulations) with those of TIP4PQ/2005 (optimized for path-integral simulations) was undertaken. A classical description of hydrates is able to correctly predict the densities at temperatures above 150 K and the relative stabilities between the hydrates and ice  $I_h$ . The inclusion of nuclear quantum effects does not significantly modify the sequence of phases found in the phase diagram of water at negative pressures, namely,  $I_h \rightarrow sII \rightarrow sH$ . In fact the transition pressures are little affected by the inclusion of nuclear quantum effects; the phase diagram predictions for hydrates can be performed with reasonable accuracy using classical simulations. However, for a reliable calculation of the densities below 150 K, the sublimation energies, the constant pressure heat capacity, and the radial distribution functions, the incorporation of nuclear quantum effects is indeed required. © 2010 American Institute of Physics. [doi:10.1063/1.3353953]

### I. INTRODUCTION

Gas hydrates are icelike inclusion compounds formed from a matrix of water that encapsulates small inert “guest” molecules, for example, Ar, Xe, H<sub>2</sub>, CH<sub>4</sub>, or CO<sub>2</sub>. Such structures are usually only stable under sufficient pressure.<sup>1,2</sup> Hydrates are classified as sI,<sup>3</sup> sII,<sup>4</sup> and sH.<sup>5</sup> The particular structure adopted depends on the guest molecule.<sup>6–8</sup> Methane hydrates are receiving significant attention given that they are a potentially important fuel source.<sup>9–17</sup> Experimentally it is not possible to study empty hydrates since they are thermodynamically unstable; the guest molecules play an important role in stabilizing these structures. However, they can be studied in computer simulations<sup>18–23</sup> since they are mechanically stable. There are several reasons to consider the study of the empty hydrates. The first is that as they are less dense than ice  $I_h$ , they could be the stable solid phases of water at negative pressures. In an earlier work,<sup>18</sup> the authors found that in classical simulations using the TIP4P/2005 model, the solid structures sII and sH become stable in this region of the phase diagram. Similar conclusions were reached by Molinero and co-workers<sup>19</sup> using a different model of water.<sup>20</sup> Second, the differences in the thermodynamic properties (in particular the chemical potential) between ice  $I_h$  and the empty

hydrates play a central role within the widely used van der Waals–Platteeuw theory.<sup>24</sup> Obviously these differences can only be estimated from theoretical calculations or from computer simulations. Finally, it is interesting to point out that the lattice parameters of hydrates are mostly determined from the host water structure; the influence of the guest molecules on the lattice parameters is small at moderate pressures.<sup>6</sup>

Since water is a relatively light molecule (the eigenvalues of the inertia tensor are small) while at the same time having strong intermolecular interactions (hydrogen bonds), one may expect that nuclear quantum effects are important.<sup>25–28</sup> This has been shown in a number of studies for liquid water<sup>28–30</sup> and in a few studies for ice  $I_h$ .<sup>31</sup> Using path-integral (PI) simulations McBride *et al.*<sup>25</sup> showed that nuclear quantum effects play a significant role in the densities and energies of many of the ice phases. Vega *et al.*<sup>32</sup> recently studied the incorporation of these quantum effects in the calculation of the heat capacity for water and ice. In view of this, performing simulations of a certain model via both classical and path-integral simulations is interesting since they illustrate the trends that can be expected to occur upon isotopic substitution (the behavior of classical water would correspond to that of very heavy isotopes).<sup>33,34</sup> These studies throw light on just how much the properties of water are affected by nuclear quantum effects. In this work we shall

<sup>a)</sup>Electronic mail: cvega@quim.ucm.es.

perform both classical and path-integral simulations of the hydrate structures sI, sII, and sH using the same model to determine the importance of nuclear quantum effects on these solids. In particular we shall use the TIP4PQ/2005 model,<sup>25</sup> which was specifically designed to reproduce the properties of ices within path-integral simulations. It will be shown that the model also provides a good description of the densities of the hydrate solids and that nuclear quantum effects are indeed quite important in the hydrate structures.

There exists another route for comparing results from classical simulations with results from path-integral simulations; instead of comparing classical and quantum simulations for the same model, one could compare classical simulations for a good classical model with quantum simulations for a good quantum model. A good classical model is one in which the parameters were fitted to experimental properties within classical simulations so that, in some implicit way, quantum contributions form part of the make-up of the model.<sup>35–38</sup> In previous work we showed that the TIP4P/2005 (Ref. 39) provides a good description of the solid phases of water, including the hydrates, when used in classical simulations.<sup>40–48</sup> Similarly it has been shown that TIP4PQ/2005 is a good water model when using path-integral simulations.<sup>25,26</sup> For example, both TIP4P/2005 and TIP4PQ/2005 reproduce the maximum in density of water, an important test for any model of water. The comparison between the results of TIP4P/2005 with classical simulations and those of TIP4PQ/2005 with PI simulations will help to clarify the limits of classical simulations when describing solid phases of water, here in particular with regard to the hydrate structures.

All said and done, it is important to point out that the two models used in this work are rigid and nonpolarizable. Obviously the inclusion of either polarizability and/or flexibility could modify somewhat the conclusions of this work. From the point of view of further improvements, it is likely that intramolecular degrees of freedom (i.e., flexibility) should be included in the model since these provide a small but probably significant contribution to intermolecular interactions. This is due to the existence of competing quantum effects (i.e., a lower dipole moment of water in the classical treatment) as discussed recently by Habershon *et al.*,<sup>49</sup> which would most likely narrow the gap between quantum and classical results. The main focus here is to investigate the importance of the interplay between the intermolecular forces (hydrogen bonding) and quantum effects related to atomic masses.

## II. METHODOLOGY

In this study classical Monte Carlo (MC) simulations were performed for both the TIP4P/2005 (Ref. 39) and the TIP4PQ/2005 (Ref. 25) models, as well as PIMC simulations for the TIP4PQ/2005 model. For the PIMC simulations the formalism of Müser and Berne for rigid bodies<sup>50,51</sup> was used. We shall describe briefly this methodology and refer the reader to the original references for further details.<sup>25,52–56</sup>

In the path-integral formulation, the canonical partition

function,  $Q_N$ , of a quantum system of  $N$  molecules (described with  $P$  Trotter slices, or “beads”) can be approximated by<sup>50,51</sup>

$$Q_N(\beta) \approx \frac{1}{N!} \left( \frac{MP}{2\pi\beta\hbar^2} \right)^{3NP/2} \int \dots \int \prod_{i=1}^N \prod_{t=1}^P d\mathbf{r}_i^t d\Omega_i^t \times \exp \left( - \frac{MP}{2\beta\hbar^2} \sum_{i=1}^N \sum_{t=1}^P (\mathbf{r}_i^t - \mathbf{r}_i^{t+1})^2 - \frac{\beta}{P} \sum_{t=1}^P U^t \right) \times \prod_{i=1}^N \prod_{t=1}^P \rho_{\text{rot},i}^{t,t+1}. \quad (1)$$

The propagator satisfies the cyclic condition that bead  $P+1$  corresponds to bead 1. Here  $\mathbf{r}_i^t$  are the Cartesian coordinates of the center of mass of replica  $t$  of molecule  $i$ , and  $\Omega_i^t$  are the Euler angles that specify its orientation.  $U_i$  is the potential energy of the replica  $t$  of the system. In this work, we use a pairwise potential ( $u_{ij}$ ) such that the potential energy of the replica  $t$  of the system is

$$U^t = \sum_i \sum_{j>i} u_{ij}(\mathbf{r}_i^t, \mathbf{r}_j^t, \Omega_i^t, \Omega_j^t). \quad (2)$$

As can be seen in Eq. (1), each replica  $t$  of molecule  $i$  interacts with the replicas of the other molecules that have the same index  $t$  via the intermolecular potential  $u_{ij}$ ; with replicas  $t-1$  and  $t+1$  of the same molecule  $i$  via a harmonic potential (connecting the center of mass  $\mathbf{r}_i^t$  of the beads of molecule  $i$ ) with a coupling parameter that depends on the mass of the molecules,  $M$ , and on the inverse temperature  $\beta$ ; and with replicas  $t-1$  and  $t+1$  of the same molecule through the terms  $\rho_{\text{rot},i}^{t-1,t}$  and  $\rho_{\text{rot},i}^{t,t+1}$ , which incorporate the quantum contribution of the rotation and that depend on the relative orientation of replica  $t$  with respect to  $t-1$ , and  $t+1$  with respect to  $t$ .

One important variable used in path-integral simulations is the number of beads ( $P$ ) (Refs. 29 and 31) employed. If  $P=1$  then the system is classical, whereas if  $P \rightarrow \infty$  then the full quantum system is retrieved. The number of beads should be chosen so that<sup>54</sup>

$$P > \frac{\hbar\omega_{\text{max}}}{k_B T}, \quad (3)$$

where  $\omega_{\text{max}}$  is the “fastest” frequency in the system of study. The number of replicas used for rigid models is lower than that used for flexible models<sup>30,49,57,58</sup> because in path-integral simulations of rigid models,<sup>31,59,60</sup> the intramolecular vibrations are neglected. For flexible models of water at 300 K, a typical number of slices is about  $P=32$ .<sup>61,62</sup> Recently a new method to reduce the computational cost for flexible systems with polarizable force fields has been developed.<sup>63</sup> We found that for a rigid model, a reasonable choice is to assume the following relation:<sup>25</sup>  $PT \approx 1500$  K. Thus in this work  $P$  ranged from 6 (at 275 K) to 20 (at 77 K) (see Table I).

The internal energy can be evaluated from

TABLE I. Number of beads ( $P$ ) or replicas in function of temperature used in the simulations. The number of  $P$  was chosen according of the relation  $PT \approx 1500$  K.

T(K)	275	250	200	150	125	100	77
$P$	6	6	8	10	12	15	20

$$E = -\frac{1}{Q_N} \frac{\partial Q_N}{\partial \beta}, \quad (4)$$

and substituting the canonical partition function [Eq. (1)] results in

$$E = K_{\text{tra}} + K_{\text{rot}} + U, \quad (5)$$

where

$$K_{\text{tra}} = \frac{3NP}{2\beta} - \left\langle \frac{MP}{2\beta^2 \hbar^2} \sum_{i=1}^N \sum_{t=1}^P (\mathbf{r}_i^t - \mathbf{r}_i^{t+1})^2 \right\rangle,$$

$$K_{\text{rot}} = \left\langle \frac{1}{P} \sum_{i=1}^N \sum_{t=1}^P \frac{\sum_{J=0}^{\infty} \sum_{M=-J}^J \sum_{\tilde{K}=-J}^J f_{J,M,\tilde{K}}^{i,t,t+1} \tilde{E}_{\tilde{K}}^{JM} \exp\left[-\frac{\beta}{P} \tilde{E}_{\tilde{K}}^{JM}\right]}{\rho_{\text{rot},i}^{t,t+1}} \right\rangle,$$

$$U = \left\langle \frac{1}{P} \sum_{t=1}^P U^t \right\rangle, \quad (6)$$

where  $\tilde{E}_{\tilde{K}}^{JM}$  are the eigenvalues of energy of the water asymmetric top, and  $f_{J,M,\tilde{K}}^{i,t,t+1}$  are some functions that depend on the relative orientation of replicas  $t$  and  $t+1$  of molecule  $i$ .<sup>25</sup>

Finally, the same methodology can be used to evaluate the partition function in the  $NpT$  ensemble

$$Q_{NpT} = A \int dV \exp(-\beta p V) Q_N, \quad (7)$$

where  $A$  is a constant with units of inverse volume so that  $Q_{NpT}$  becomes dimensionless.

The location of the oxygens in the initial solid configurations for sI, sII, and sH were obtained from crystallographic data.<sup>64</sup> The simulation box contained  $2 \times 2 \times 2$  unit cells, with a total of 368 and 1088 molecules for the cubic structures sI and sII, respectively. For the sH (hexagonal symmetry), we used a  $3 \times 2 \times 2$  supercell, which contained 408 water molecules. The number of molecules used for ice  $I_h$  was 432. All these structures present proton disorder.<sup>65–68</sup> We used the algorithm proposed by Buch *et*

*al.*<sup>69</sup> to generate proton disordered structures satisfying the Bernal–Fowler rules<sup>70</sup> and with zero (or almost zero) dipole moment.

As mentioned at the beginning of this section, two water models were employed to describe the interaction between water molecules; TIP4P/2005 (Ref. 39) and TIP4PQ/2005;<sup>25</sup> the parameters for both of them are provided in Table II. The models differ only in the value of the charge (slightly larger in the TIP4PQ/2005). The increase in the charge compensates (to some extent) for the increase in the energy due to quantum effects. It has been shown in previous work that PI simulations of TIP4PQ/2005 reproduce the temperature of maximum density of water,<sup>26</sup> the density of the solid phases,<sup>25</sup> and the radial distribution functions of ice  $I_h$  (Ref. 25) and liquid water.<sup>26</sup>

Anisotropic  $NpT$  simulations<sup>71,72</sup> (Parrinello–Rahman-like) were used both for classical MC and PIMC simulations. In both methods and for both water models, the pair potential was truncated at 8.5 Å for all phases, and standard long-range corrections to the Lennard-Jones energy and pressure were added.<sup>56,73</sup> Ewald sums were employed for the electrostatic interactions with the real part of the electrostatic contribution truncated at 8.5 Å. The simulations consisted of a total of 100 000 MC cycles (a trial move per particle plus a trial volume change) of which 30 000 were used for equilibration and the remaining cycles to evaluate averages.

### III. RESULTS

If the lattice parameters of the unit cell are known from experiment, then the “experimental” density of the empty gas hydrate can be estimated as being

$$\rho_{\text{expt}} = \frac{n_{\text{H}_2\text{O}} M}{N_{\text{AV}} V_c} \quad (8)$$

where  $n_{\text{H}_2\text{O}}$  is the number of water molecules per unit cell in the hydrate structure (sI, sII, or sH),  $M$  is the molecular weight,  $N_{\text{AV}}$  is the Avogadro’s number, and  $V_c$  is the volume of the unit cell. In Table III the experimental lattice parameters<sup>74–78</sup> for two different temperatures are given. The experimental densities of the empty gas hydrate as estimated

TABLE II. Parameters for both the TIP4PQ/2005 (Ref. 25) and the TIP4P/2005 (Ref. 39) models. The distance between the oxygen and hydrogen sites is  $d_{\text{OH}}$ . The angle, in degrees, formed by hydrogen, oxygen, and the other hydrogen atom is denoted by  $\angle \text{H-O-H}$ . The Lennard-Jones site is located on the oxygen with parameters  $\sigma$  and  $\epsilon$ . The charge on the proton is  $q_{\text{H}}$ . The negative charge is placed on a point M at a distance  $d_{\text{OM}}$  from the oxygen along the H-O-H bisector.

Model	$d_{\text{OH}}$ (Å)	$\angle \text{H-O-H}$	$\sigma$ (Å)	$\epsilon/k_B$ (K)	$q_{\text{H}}$ (e)	$d_{\text{OM}}$ (Å)
TIP4P/2005	0.9572	104.52	3.1589	93.2	0.5564	0.1546
TIP4PQ/2005	0.9572	104.52	3.1589	93.2	0.5764	0.1546

TABLE III. Experimental lattice parameters at normal pressure for two different temperatures. The experimental density is estimated from Eq. (8). Lattice parameters are given in angstrom.  $\rho$  is given in  $\text{g cm}^{-3}$ . The number of molecules in the sI, sII, and sH unit cells are 46, 136, and 34, respectively.

Phase	Lattice parameters	$\rho_{\text{expt}}$	$\rho_{\text{TIP4PQ/2005}}$
T=200 K			
sI	(a=11.91) <sup>a</sup>	0.815	0.815
sII	(a=17.17) <sup>b</sup>	0.804	0.803
sH	(a=12.28; c=10.08) <sup>c</sup>	0.773	0.784
T=100 K			
sI	(a=11.875) <sup>d</sup>	0.822	0.819
sII	(a=17.11) <sup>b</sup>	0.812	0.807
sH	(a=12.20; c=10.01) <sup>c</sup>	0.788	0.788

<sup>a</sup>References 74–77.

<sup>b</sup>Reference 78.

<sup>c</sup>Reference 74.

<sup>d</sup>Reference 77.

from Eq. (8) are also presented. Obviously the unit cell parameters depend on temperature,<sup>74,77</sup> and thus so does the density. As can be seen the densities of the empty hydrates are lower than that of ice  $I_h$  (which is about<sup>79</sup>  $0.92 \text{ g/cm}^3$ ), and for this reason these phases are ideal candidates to occupy the phase diagram of water at negative pressures<sup>18</sup> (i.e., at constant temperature any phase transition always decreases the density when decreasing the pressure, as stated by Bridgmann<sup>80</sup>).

### A. Nuclear quantum effects in the empty gas hydrates

In Table III the densities of the different empty hydrates as obtained from PI simulations of the TIP4PQ/2005 are presented. One can see that the predicted densities agree quite

well (to within 0.5%) with the experimental values. Thus the TIP4PQ/2005 model is able to describe not only the densities of the solid phases of water (ices)<sup>25</sup> but also those of the hydrate structures. To analyze the importance of nuclear quantum effects in hydrates, we have also performed classical simulations using the same model. The results of these classical simulations of the TIP4PQ/2005 model are labeled as TIP4PQ/2005<sub>(classical)</sub>.

The results are presented in Table IV. The densities of the classical simulations are about  $\approx 0.03 \text{ g/cm}^3$  higher than their quantum counterparts. The potential energies of the PI simulations are about  $\approx 1.5 \text{ kcal/mol}$  higher than those obtained from classical simulations. The total kinetic energy is higher in the PI simulations (by about  $\approx 1.3 \text{ kcal/mol}$ ) than in the classical simulations. The kinetic energy in the classical simulations is twice  $(3/2)RT$  since both translational and rotational degrees of freedom contribute  $(3/2)RT$ . Notice that the PI translational energies are slightly larger than  $(3/2)RT$ , but the PI rotational energies are substantially larger than  $(3/2)RT$ . This clearly indicates that nuclear quantum effects in water arise mostly from the hindered rotation of the molecule due to the formation of hydrogen bonds. The rotational kinetic energy is hardly affected by the temperature, so it does not contribute much to the heat capacity. The rotational energy obtained for the hydratelike structures is similar to that obtained for ice  $I_h$ , but it is slightly different from that found for ices II and V. Rotational quantum effects are slightly larger in the phases sI, sII, sH, and  $I_h$  (i.e., higher rotational energies compared to the classical value) than in ices II and V. This may be due to the different arrangement of molecules within the first coordination layer, which is an almost perfect tetrahedron for the low dense ices ( $I_h$ , sI, sII, and sH) and a distorted tetrahedron for the high density ices (II and V). We shall return later to this point. The total inter-

TABLE IV. Results from PI simulations using the TIP4PQ/2005<sub>(PI)</sub> model for the empty hydrates (sI, sII, and sH) and for a series of solid phases (ice  $I_h$ , II, and V). The results from classical simulations for the same model are also included. All energies are in units of kcal/mol, and the densities are in  $\text{g cm}^{-3}$ . The classical value of the kinetic translational or rotational energy  $(3/2)RT$  is also provided for comparison. The values for ices  $I_h$ , II, and V are taken from the work of McBride *et al.* (Ref. 25), except  $U_{\text{(classical)}}$  and  $\rho_{\text{(classical)}}$  that have been calculated in this work.

Phase	$T$ (K)	$p$ (bar)	$(3/2)RT$	$K_{\text{transl.}}$	$K_{\text{rot.}}$	$K_{\text{total}}$	$U$	$E$	$U_{\text{(classical)}}$	$\rho_{\text{(PI)}}$	$\rho_{\text{(classical)}}$
sI	125	1	0.38	0.54	1.41	1.95	-13.98	-12.04	-15.42	0.818	0.848
sI	100	1	0.30	0.50	1.41	1.91	-14.04	-12.13	-15.58	0.819	0.851
sI	77	1	0.23	0.46	1.42	1.88	-14.08	-12.20	-15.73	0.819	0.854
sII	125	1	0.38	0.54	1.42	1.96	-14.01	-12.05	-15.44	0.807	0.836
sII	100	1	0.30	0.50	1.42	1.92	-14.07	-12.15	-15.61	0.807	0.839
sII	77	1	0.23	0.46	1.42	1.89	-14.11	-12.22	-15.75	0.807	0.842
sH	125	1	0.38	0.54	1.41	1.95	-13.91	-11.96	-15.33	0.788	0.817
sH	100	1	0.30	0.50	1.40	1.90	-13.97	-12.06	-15.50	0.788	0.820
sH	77	1	0.23	0.47	1.42	1.89	-14.01	-12.13	-15.65	0.788	0.822
$I_h$	125	1	0.38	0.54	1.41	1.96	-14.25	-12.29	-15.68	0.928	0.960
$I_h$	100	1	0.30	0.50	1.42	1.92	-14.32	-12.40	-15.85	0.928	0.963
$I_h$	77	1	0.23	0.46	1.43	1.89	-14.34	-12.45	-15.99	0.927	0.966
II	125	1	0.38	0.53	1.32	1.84	-14.06	-12.21	-15.36	1.185	1.223
II	100	1	0.30	0.48	1.30	1.78	-14.14	-12.35	-15.52	1.188	1.230
II	77	1	0.23	0.44	1.32	1.76	-14.16	-12.40	-15.67	1.190	1.235
V	125	1	0.38	0.53	1.34	1.84	-13.80	-11.93	-15.15	1.248	1.289
V	100	1	0.30	0.49	1.34	1.82	-13.88	-12.06	-15.31	1.251	1.296
V	77	1	0.23	0.44	1.35	1.79	-13.91	-12.12	-15.46	1.253	1.302

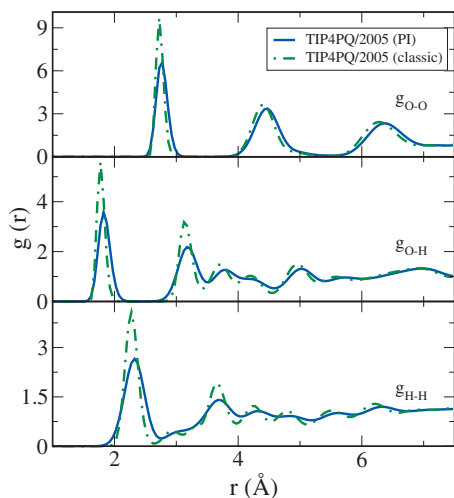


FIG. 1. Radial distribution function of sI hydrate described with the TIP4PQ/2005 model as obtained from PI simulations (solid blue line) and from classical simulations (dashed dotted green line) at 100 K and 1 bar.

nal energy of the quantum system is about 2.6 kcal/mol higher than that of the classical system at 125 K and about 3.1 kcal/mol higher at 77 K (half of the difference arising from the potential energy and the other half from the kinetic energy). A rough estimate of the difference at 0 K would yield 3.8 kcal/mol, which would correspond approximately to the zero point energy of the model. For ice  $I_h$ , Whalley<sup>81</sup> estimated the zero point energy to be about 3.94 kcal/mol, which is similar to the value reported here. Thus for the TIP4PQ/2005 the zero point energies of the phases  $I_h$ , sI, sII and sH are quite similar; about 3.8 kcal/mol.

We shall now consider the impact of nuclear quantum effects on the structure. In Fig. 1 the radial distribution functions (O–O, O–H, and H–H) of the sI hydrate as obtained from classical and quantum simulations of the TIP4PQ/2005 model are presented. The peaks of the classical simulations are shifted to lower distances, reflecting the higher density of the system. The second difference is the higher values of the peaks (especially the first peak) in the classical simulations. The differences are higher for the O–H and H–H distribution functions. Obviously the nuclear quantum effects affect more significantly the correlation functions in which the hydrogen atom is involved. The results in Fig. 1 illustrate the trend that may be expected in the structure when replacing the atoms of the water molecule by heavier isotopes.

Finally we shall consider the relative energies between ices at zero temperature and pressure. Path-integral simulations cannot be performed at very low temperatures (since one would have to use a prohibitively large number of beads). According to the third law of thermodynamics,<sup>82</sup> the heat capacity must approach zero as the temperature is decreased. In previous work<sup>25</sup> we used a fit of the form  $H = a_0 + a_1 T^4$ , which satisfies both the third law and the Debye law, i.e.,  $C_p \propto T^3$ . However, when analyzing the experimental values of the heat capacity of ice  $I_h$ , we found that the Debye law applies only for temperatures below 15 K. Also the experimental enthalpies up to the melting temperature are described much better by a cubic polynomial (with no linear term in temperature). In view of this we shall use  $H = a_0$

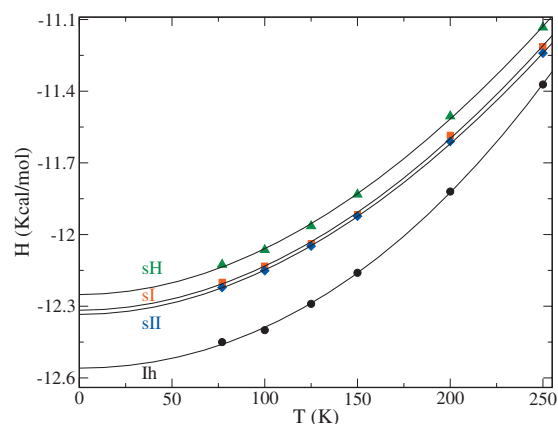


FIG. 2. Enthalpy of empty hydrates and ice  $I_h$  at low temperatures and at  $p=1$  bar for the TIP4PQ/2005 model as obtained from PI simulations. Lines correspond to the fit  $H = a_0 + a_1 T^2 + a_2 T^3$ . The error in the enthalpy is of the order  $\pm 0.04$  kcal/mol. The values for ice  $I_h$  were taken from McBride *et al.* (Ref. 25).

$+ a_1 T^2 + a_2 T^3$ . By fitting the enthalpies of the hydrates and of the ices calculated from PI simulations at 250, 200, 150, 125, 100, and 77 K ( $p=1$  bar), the parameters  $a_0$ ,  $a_1$ , and  $a_2$  are obtained. The results of the fit for ice  $I_h$ , sI, sII, and sH are presented in Fig. 2. The parameter  $a_0$  represents the enthalpy of the solid phase at zero temperature and normal pressure. Basically the enthalpy at normal pressure and zero temperature  $H(T=0, p=1 \text{ bar})$  is almost identical to the internal energy at zero temperature and pressure  $E(T=0, p=0 \text{ bar})$  since the contribution of the  $pV$  term is about five orders of magnitude smaller than the internal energy term, and besides, the internal energy is hardly affected by a change in pressure from 0 to 1 bar. The error introduced by this approximation is smaller than 0.0001 kcal/mol. Therefore in this work we shall use the approximation  $H(T=0, p=1 \text{ bar}) = E(T=0, p=0 \text{ bar})$ . The energies at 0 K and 0 bar obtained from classical simulations were calculated by performing  $NpT$  simulations at several temperatures below 100 K and fitting the results for the internal energy to a straight line. In Table V the energies at 0 K and zero pressure obtained from classical and quantum simulations of the TIP4PQ/2005 model are presented. The classical and quantum 0 K energies are quite different, reflecting the fact that the quantum simulations include the zero point energy, which is absent in the classical simulations, which, at 0 K, provide only the lattice energy. Also in Table V the relative energies (with respect to ice  $I_h$ ) for these two types of simulations are presented.

The relative energies of the hydrates (sI, sII, and sH) with respect to ice  $I_h$  obtained from classical and path-integral simulations are similar, suggesting that for the low dense solid structures ( $I_h$ , sI, sII, and sH), nuclear quantum effects affect in a similar manner to these type of solids. However, the relative energies of ices II, III, V, and VI with respect to ice  $I_h$  are different in classical and path-integral simulations, suggesting that nuclear quantum effects affect in a slightly different manner the low and the high density solid phases of water.

TABLE V. Comparison of the energies  $E$  and densities  $\rho$  at 0 K and zero pressure for the empty hydrates and for a series of solid phases for the TIP4PQ/2005 model as obtained from classical simulations and from PI simulations. The energies are in units of kcal/mol, and the densities are in units of  $\text{g cm}^{-3}$ . The lowest energy (most stable phase) is shown in bold font. The energies at 0 K for TIP4PQ/2005 model from PI simulations are slightly different to those from work McBride *et al.* (Ref. 25) due to the different analytical expressions used to fit the simulation results. The lower section provides the relative energies with respect to ice  $I_h$ . The errors (in kcal/mol) are  $\mathcal{O}(0.02)$  in  $E$  and consequently  $\mathcal{O}(0.04)$  in the relative energy. The error for the density is  $\mathcal{O}(0.002)$  in  $\text{g cm}^{-3}$ .

Phase	TIP4PQ/2005 <sub>(classical)</sub>		TIP4PQ/2005 <sub>(PI)</sub>	
	$\rho$ (0 K)	$E$ (0 K)	$\rho$ (0 K)	$E$ (0 K)
$I_h$	0.974	<b>-16.49</b>	0.927	<b>-12.56</b>
sI	0.863	-16.21	0.819	-12.32
sII	0.851	-16.24	0.807	-12.33
sH	0.831	-16.14	0.788	-12.24
II	1.254	-16.15	1.190	-12.54
III	1.197	-16.08	1.146	-12.32
V	1.321	-15.94	1.253	-12.25
VI	1.412	-15.78	1.336	-12.11

Phase	TIP4PQ/2005 <sub>(classical)</sub>		TIP4PQ/2005 <sub>(PI)</sub>	
	$\Delta E$ (0 K)		$\Delta E$ (0 K)	
$I_h$	<b>0</b>		<b>0</b>	
sI	0.27		0.24	
sII	0.24		0.22	
sH	0.35		0.32	
II	0.34		0.02	
III	0.41		0.24	
V	0.55		0.31	
VI	0.71		0.45	

## B. Classical and quantum descriptions of empty gas hydrates

From the results presented thus far, it is clear that nuclear quantum effects are important when studying empty gas hydrates. This situation could change if one compares results from a model optimized for classical simulations (TIP4P/2005) with another model optimized for PI simulations (TIP4PQ/2005). It may be the case that the change in the potential parameters of the rigid classical nonpolarizable model (with respect to the quantum model) incorporates, in a mean field like way, the impact of the nuclear quantum effects. This might be regarded as a sort of empirical counterpart to the Feynman–Hibbs analytic approach,<sup>52,83,84</sup> although in the latter, one performs classical-like simulations using a temperature-dependent effective potential, and this temperature dependence on the pair interaction is lost when using the TIP4P/2005 model. In what follows it should be implicit that any result for TIP4P/2005 was obtained using classical simulations, whereas any result for TIP4PQ/2005 was obtained from PI simulations.

In Table VI the densities of both models at 200 and 100 K are presented and compared to the experimental data. It can be seen that at 200 K, both models yield quite good predictions. At 100 K both models yield reasonable results, although it seems that the densities of TIP4P/2005 are some-

TABLE VI. Densities for sI, sII, and sH hydrates at normal pressure as obtained from simulation and compared with the experimental density as obtained by Eq. (8) from experimental lattice parameters.

Phase	TIP4P/2005	TIP4PQ/2005	$\rho_{\text{expt}}$
T=200 K			
sI	0.819	0.815	0.815
sII	0.807	0.803	0.804
sH	0.788	0.784	0.773
T=100 K			
sI	0.832	0.819	0.822
sII	0.821	0.807	0.812
sH	0.801	0.788	0.788

what larger than the experimental values. Not surprisingly, when the temperature decreases the importance of nuclear quantum effects increases. We have computed the density from 3 to 275 K for TIP4P/2005 and from 77 to 275 K for TIP4PQ/2005. The results for the sI hydrate are presented in Fig. 3. For TIP4P/2005 the density increases as the temperature decreases all the way down to 0 K. For TIP4PQ/2005 the density increases as the temperature decreases, but for temperatures below 125 K, the density does not change much with temperature. Experimentally one finds that there is very little variation in the density of ice  $I_h$  in the temperature range of 0–125 K, and one may expect a similar behavior for the hydrates (although in a smaller temperature range<sup>9</sup>). Classical simulations are unable to capture this. In summary TIP4P/2005 can satisfactorily describe the densities of the hydrates at temperatures above 150 K, but it fails at temperatures below 150 K since classical simulations do not capture one of the consequences of the third law of thermodynamics (i.e., the thermal expansion coefficient,  $\alpha$ , should go to zero at 0 K).

In Fig. 4 the radial distribution functions of sI hydrate at 100 K and 1 bar as described by the TIP4PQ/2005 and TIP4P/2005 models are presented. The location of the peaks is similar for both models (reflecting that both models predict similar densities). However the peaks of the TIP4P/2005 are higher than those of TIP4PQ/2005. There are no experimen-

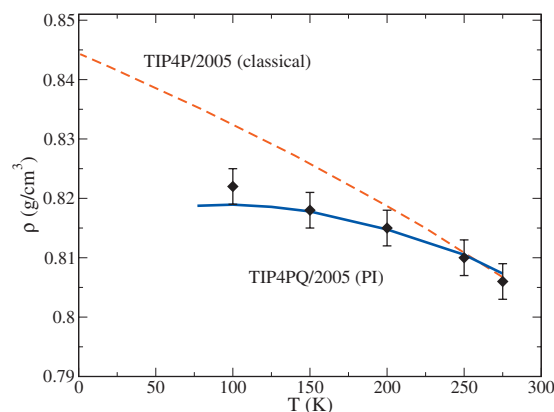


FIG. 3. Equation of state for sI at  $p=1$  bar predicted by the classical TIP4P/2005 model (red dashed line) and the TIP4PQ/2005 model (blue solid line). Experimental values (diamond symbol) calculated from the experimental lattice parameters taken from Refs. 74–78 are also shown.

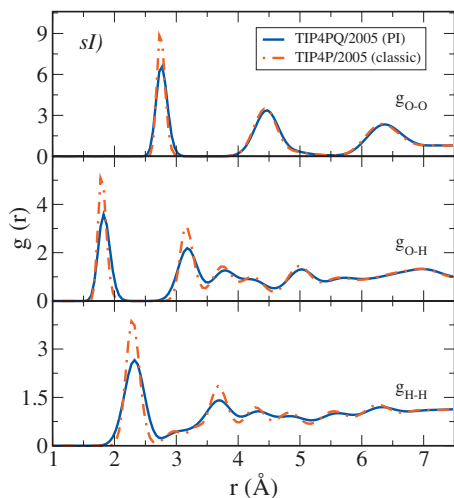


FIG. 4. Radial distribution function of sI hydrate as obtained for TIP4PQ/2005 from PI simulations (solid blue line) and for TIP4P/2005 from classical simulations (dashed dotted red line) at 100 K and 1 bar.

tal results for the radial distribution functions of hydrates to judge which model yields a better agreement with experiment. However in previous work we found that the structural predictions for ice  $I_h$  and water for TIP4PQ/2005 (Refs. 25 and 26) were in better agreement with experiment than those of TIP4P/2005.<sup>39,47</sup> It is reasonable to assume that the same occurs for the hydrates. For this reason it is clear that a rigid classical nonpolarizable model cannot provide a quantitative description of the structure of the hydrates and/or ices. The same applies to the fluid phase.<sup>26</sup> Although the qualitative description of the structure provided by the rigid classical nonpolarizable model is reasonable, one has the feeling that a classical effective model can never reproduce quantitatively the experimental structure of water (as given by the radial distribution functions), and when it does this is probably due to the fact that the potential parameters were selected to force such agreement, most likely spoiling the predictions of the model for a number of other properties. The same behavior was found for the sII and sH hydrates. Their radial distribution functions are presented in Figs. 5 and 6, respectively. It is not surprising that similar values are found for the  $g(r)$  of the sI and sII structures since these structures are formed by the same type of cavity ( $5^{12}$  and  $5^{12}6^2$ ) although in different proportions. The results of the  $g(r)$  for the sH structure are slightly different because in addition to being formed by the cavity  $5^{12}$ , it is also composed of the cavities  $4^35^66^3$  and  $5^{12}6^8$ .

Let us now discuss the properties of the ices at zero temperature and pressure. For TIP4P/2005 these properties have been reported by Aragonés *et al.*<sup>85</sup> for ices and by Conde *et al.*<sup>18</sup> for hydrates. For TIP4PQ/2005 they were obtained by fitting the enthalpies at normal pressure obtained from PI simulations at 250, 200, 150, 125, 100, and 77 K ( $p=1$  bar) to the expression  $H=a_0+a_1T^2+a_2T^3$  and determining the value of the parameter  $a_0$ . Values of the enthalpies are given as electronic supplementary information<sup>86</sup> (notice that the energies at 0 K and zero pressure reported here for ices  $I_h$ , II, III, V, and VI differ by about 0.10 kcal/mol from those reported in our previous work<sup>25</sup> due to the differ-

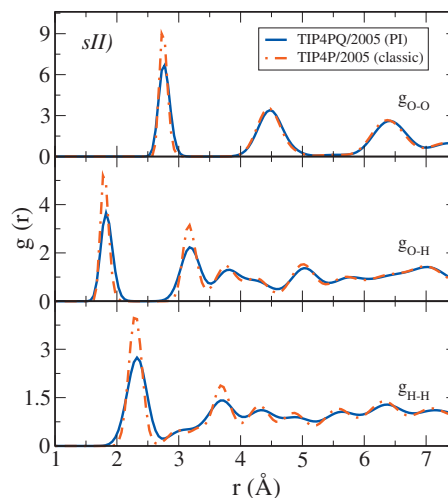


FIG. 5. Radial distribution function of sII hydrate as obtained for TIP4PQ/2005 from PI simulations (solid blue line) and for TIP4P/2005 from classical simulations (dashed dotted red line) at 100 K and 1 bar.

ent expression used to fit the enthalpies and to the fact that here results for six different temperatures were used in the fit, whereas only three were used in our previous work). The estimated values of the energies at 0 K are given in Table VII for TIP4P/2005 and TIP4PQ/2005. The energies of TIP4PQ/2005 are about 2.5 kcal/mol higher than those of TIP4P/2005 (this difference arises from the absence of zero point energy in the TIP4P/2005, which amounts to about 3.8 kcal/mol, the difference being partially compensated by the larger value of the charges in TIP4PQ/2005 with respect to TIP4P/2005). The experimental sublimation enthalpy at 0 K of ice  $I_h$  (Refs. 79 and 81) is about 11.31 kcal/mol. The TIP4P/2005 model would predict 15.059 kcal/mol. The sublimation enthalpy of ice  $I_h$  for TIP4PQ/2005 is found to be 12.57 kcal/mol, which is much closer to the experimental result. This improvement is due to the fact that the TIP4PQ/2005 includes the zero point energy, which becomes an important contribution at 0 K (we estimate that it is about 3.8 kcal/mol for the solid phases considered in this work). For a nonpolarizable model,

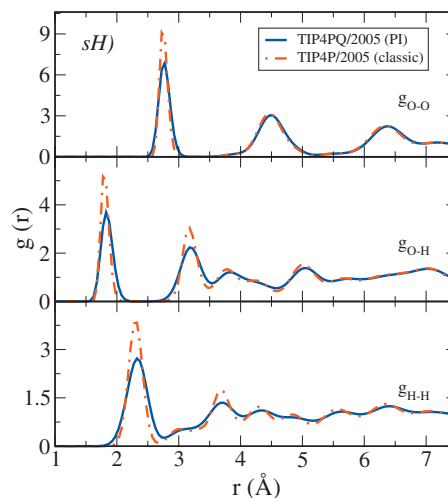


FIG. 6. Radial distribution function of sH hydrate as obtained for TIP4PQ/2005 from PI simulations (solid blue line) and for TIP4P/2005 from classical simulations (dashed dotted red line) at 100 K and 1 bar.

TABLE VII. Comparison of the energies,  $E$ , at 0 K and zero pressure for the empty hydrates for both the TIP4P/2005 and the TIP4PQ/2005 models. The energies are in units of kcal/mol. The lowest energy (most stable phase) is shown in bold font. The lower section provides the relative energies with respect to ice  $I_h$ . The values for the TIP4P/2005 model are taken from the work of Conde *et al.* (Ref. 18) and Aragonés *et al.* (Ref. 85). The error (in kcal/mol) is  $\mathcal{O}(0.02)$  in  $E$  and consequently  $\mathcal{O}(0.04)$  in the relative energy.

Phase	$E$ (0 K estimate)	
	TIP4P/2005	TIP4PQ/2005
$I_h$	<b>-15.06</b>	<b>-12.56</b>
sI	-14.82	-12.32
sII	-14.84	-12.33
sH	-14.74	-12.24
II	-14.85	-12.54
III	-14.74	-12.32
V	-14.64	-12.25
VI	-14.51	-12.11
$I_h$	<b>0</b>	<b>0</b>
sI	0.24	0.24
sII	0.22	0.22
sH	0.32	0.32
II	0.21	0.02
III	0.32	0.24
V	0.42	0.31
VI	0.55	0.45

it makes sense to apply a self-polarization correction as proposed by Berendsen<sup>87</sup> to the sublimation enthalpy. For the TIP4PQ/2005 the polarization correction would amount to approximately 1.3 kcal/mol. Including the self-polarization term to the sublimation enthalpy of ice  $I_h$  as obtained with the TIP4PQ/2005 model would yield a value of 11.27 kcal/mol, which is in excellent agreement with the experimental value of 11.31 kcal/mol. Thus the TIP4PQ/2005 is able to reproduce the sublimation enthalpy and the vaporization enthalpy<sup>26</sup> when Berendsen's correction is applied. Notice that the TIP4P/2005 was also able to reproduce the vaporization enthalpy of water when using the Berendsen's correction.<sup>39</sup> However TIP4P/2005 fails completely in describing sublimation enthalpies of ice  $I_h$  and hydrates. Quantum effects are too strong and one cannot simply disregard them. The message is that a classical treatment cannot describe sublimation enthalpies of the solid phases of water.

In Table VII the relative energies are also presented. As can be seen for the low dense solids ( $I_h$ , sI, sII, and sH), the relative energies obtained by TIP4P/2005 and TIP4PQ/2005 are quite similar. The values reported here are also similar to those reported by Koyama *et al.* for the chemical potential difference between  $I_h$ -sI and  $I_h$ -sII using the TIP4P model.<sup>88</sup> However the relative energies of the high dense ices (II, III, V, and VI) with respect to ice  $I_h$  obtained with the TIP4P/2005 are somewhat different from those of TIP4PQ/2005. Thus, nuclear quantum effects affect in a different manner low and high density ices. Why is the stability between ice  $I_h$  and the hydrates or between the hydrates themselves uninfluenced by nuclear quantum effects? The reason may be in the geometrical arrangement of the four water molecules that are forming hydrogen bonds with a central one. In ice  $I_h$ ,

TABLE VIII. Coexistence pressures (in bar) for the TIP4PQ/2005 model estimated at 0 K by using Eq. (9). The values for the classical TIP4P/2005 model are taken from Ref. 18. The sequence of stability is  $I_h \rightarrow$  sII  $\rightarrow$  sH at negative pressures and  $I_h \rightarrow$  II  $\rightarrow$  VI at positive pressures for both models. The values in bold font correspond to the stable transitions. The error in the pressure is given in parentheses. The data for the coexistence pressures of the ices for the TIP4PQ/2005 are slightly different to those reported in the work of McBride *et al.* (Ref. 25) due to the different analytical expression used to fit the simulation results to obtain the energy at 0 K.

Phases	TIP4P/2005	TIP4PQ/2005	Expt.
$I_h$ -sI	-4174	-3948 (700)	...
$I_h$ -sII	<b>-3379</b>	<b>-3249 (600)</b>	...
$I_h$ -sH	-4072	-3933 (500)	...
sII-sI	2787	2267 (3000)	...
sII-sH	<b>-7775</b>	<b>-7557 (2000)</b>	...
$I_h$ -II	<b>2090</b>	<b>195 (500)</b>	<b>140 (200)</b>
$I_h$ -III	3630	2727 (500)	2400 (100)
II-V	11 230	15 731 (2000)	18 500 (4000)
II-VI	<b>8530</b>	<b>10 935 (1000)</b>	<b>10 500 (1000)</b>
III-V	3060	1998 (1000)	3000 (100)
V-VI	6210	6848 (1000)	6200 (200)

these four molecules essentially form a perfect tetrahedron. In the hydrates the four nearest neighbors form a slightly distorted tetrahedron.<sup>1,89-91</sup> Deviations from a perfect tetrahedron in hydrates are quite small ( $\pm 10^\circ$ ) when compared to the deviations found in other ices such as ice II, III, V, and VI (Refs. 25 and 92) ( $\pm 30^\circ$ ). This should be sufficient to understand why the relative stability of empty hydrates respect to ice  $I_h$  does not change when quantum effects are introduced; the change in energy in all these structures ( $I_h$ , sI, sII, and sH) is almost the same, and therefore the stability is not affected by the quantum contribution. In the high density ices the molecules that form hydrogen bonds with a central are arranged in a highly distorted tetrahedron, resulting in weaker hydrogen bonds. That explains why nuclear quantum effects are slightly smaller in ices II, III, V, and VI when compared to  $I_h$ , sI, sII, and sH, affecting the relative energy of the high density ices with respect to ice  $I_h$ .

Once the properties of the solid water phases at zero temperature and pressure are known, one can obtain a good estimate of the phase transitions at 0 K. This idea was suggested by Whalley<sup>81</sup> in the 1980s. The transition pressure between two solid structures at 0 K can be estimated by using the following equation:

$$p_{\text{eq}} = \left. \frac{-\Delta U}{\Delta V} \right|_{p=0}. \quad (9)$$

This equation was denoted as the zero-order approximation in our previous work<sup>85</sup> and provides a quick route to estimate transition pressures between solid phases at 0 K. This equation requires only the knowledge of the densities and energies of the solids at zero temperature and pressure. We have tested that the transition pressures at 0 K obtained from this simple approach are in excellent agreement with those obtained from more sophisticated free energy calculations.<sup>85</sup> In Table VIII the coexistence pressures as estimated from the zero-order approximation are given. For the TIP4PQ/2005 we shall assume that the density at 0 K is

identical to that obtained at 77 K (quantum simulations satisfy the third law of thermodynamics, and therefore density changes are quite small below 100 K). For the TIP4P/2005 the properties at 0 K and 0 bar have been reported previously.<sup>18</sup> As expected the coexistence pressures are similar for both models. For the TIP4P/2005 the transition from  $I_h$  to sII occurs at  $-3379$  bar, followed by the transition from sII to sH at  $-7775$  bar. The sequence of stability is  $I_h \rightarrow sII \rightarrow sH$  at negative pressures. The sI phase is not thermodynamically stable at 0 K. For the TIP4PQ/2005 model the transition from  $I_h$  to sII occurs at  $-3249$  bar, followed by the transition from sII to sH at approximately  $-7557$  bar. The sequence of stability is  $I_h \rightarrow sII \rightarrow sH$ . As can be seen the ordering of phases and the transition pressures are similar both for TIP4P/2005 and for TIP4PQ/2005. In summary nuclear quantum effects do not affect much the transition pressures between the low dense solids. However, the transition pressure between ice  $I_h$  and ice II is affected significantly (and the same is true to a less extent for the  $I_h$ -III transition). The  $I_h$ -II and  $I_h$ -III transition pressures are lower in TIP4PQ/2005 than in TIP4P/2005, just reflecting the higher impact of quantum effects on ice  $I_h$  when compared to ices II and III (we already pointed out when discussing the results of Table IV, the higher value of the rotational energy of ice  $I_h$  with respect to ice II, indicating higher nuclear quantum effects for the former). Concerning the other transitions it is seen that nuclear quantum effects do not modify much the value of the III-V and V-VI transitions. However the II-V and II-VI transitions are also affected significantly by nuclear quantum effects moving to higher pressures in the quantum system. This just reflects the higher importance of nuclear quantum effects for ices V and VI when compared to ice II (which could be hinted from the higher rotational energy of ice V when compared to that of ice II, as it can be seen in the results of Table IV). It is worth pointing out that ice II is the only structure considered in this work where the protons are ordered. The experimental values of the transition pressures are also shown in the last column of Table VIII. As it can be seen the predictions of TIP4PQ/2005 are in better agreement with experiment than those of TIP4P/2005. Thus the inclusion of nuclear quantum effects improves the description of the experimental results.

Finally, once we know the enthalpy of the hydrates and of several ices at different temperatures, it is possible estimate the heat capacity via

$$C_p = \left( \frac{\partial H}{\partial T} \right)_p. \quad (10)$$

For the PI simulations we used a fit of the form  $H = a_0 + a_1 T^2 + a_2 T^3$ , whereas for the classical simulations we fitted the enthalpy to an expression of the form  $H = a_0 + a_1 T + a_2 T^2$  (of course, the classical expression does not satisfy the third law). The heat capacity as function of the temperature for the sI hydrate and ice  $I_h$  (Ref. 32) is shown in Fig. 7 (upper panel) as obtained from classical and path-integral simulations. The predictions from both types of simulations differ notably, and the largest deviations are found at the lower temperatures. For the classical simulations the  $C_p$  does not approach zero as the temperature is decreased, thus violating

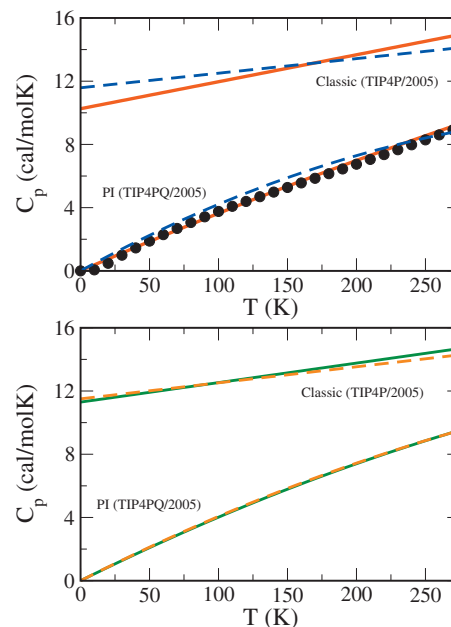


FIG. 7. Constant pressure heat capacity  $C_p$  at normal pressure as function of the temperature for classical simulations (TIP4P/2005) and PI simulations (TIP4PQ/2005). Upper graph sI hydrate and ice  $I_h$ . The dashed blue line corresponds to the values for ice  $I_h$  and the solid red line to those for sI hydrate. The values for ice  $I_h$  as obtained from computer simulations were taken from Ref. 32. Experimental results (circle symbol) for ice  $I_h$  were taken from Ref. 79. Lower graph results for ices II (dashed orange line) and V (solid green line).

the third law of thermodynamics. In literature there is no experimental data for  $C_p$  for empty hydrates since these are not thermodynamically stable. For that reason we compare our results with the experimental heat capacities for ice  $I_h$  reported by Feistel and Wagner.<sup>79</sup> The heat capacities of ice  $I_h$  and sI obtained from path-integral simulations are quite similar (being the values of ice  $I_h$  slightly larger) and are in reasonable agreement with the experimental values for ice  $I_h$ . In Fig. 7 (lower panel), the heat capacities as function of the temperature for ices II and V are shown. As before the classic treatment of the heat capacity violates the third law of thermodynamics. In the results obtained from PI simulations, the  $C_p$  approaches zero as the temperature is decreased. The heat capacities of ices II and V are quite similar and slightly larger than those found in our quantum simulations of  $I_h$  and sI. In summary the values of  $C_p$  at normal pressure found for ices  $I_h$ , sI, II, and V are quite similar and seem to increase slightly with the density of the solid structure. Therefore we can conclude that this property is particularly affected by quantum effects, and a classical treatment of this property is incorrect for all temperatures up to the melting point, in agreement with the results obtained recently for water and ice  $I_h$  by Vega *et al.*<sup>32</sup>

## IV. CONCLUSIONS

In this work PI simulations of the TIP4PQ/2005 model have been performed for the hydrate structures sI, sII, and sH. The main conclusions are as follows.

- The TIP4PQ/2005 model is able to correctly predict the densities of the hydrate solids.

- By performing both classical and PI simulations of the TIP4PQ/2005 model, it has been shown that nuclear quantum effects modify the density of the hydrates by about  $0.03 \text{ g/cm}^3$ , the total energy by about 3 kcal/mol (half of the contribution due to the potential energy and the other half to the kinetic energy), and significantly modify the structure of the hydrates. The zero point energy of the TIP4PQ/2005 is estimated to be about 3.8 kcal/mol for ice  $I_h$ , sI, sII, and sH. Absolute energies of the solids obtained from the classical and quantum treatment are quite different, but the relative energies between  $I_h$  and the sI, sII, and sH structures are rather similar. Ice  $I_h$  becomes slightly more unstable with respect to sI, sII, and sH when using a quantum description. Overall, comparing classical and quantum simulations of the same model, it is clear that there are substantial differences, indicating the importance of quantum effects in water. Therefore, nuclear quantum effects should be taken into account to quantitatively describe hydrates when using the true potential energy surface obtained from first principle calculations.<sup>93-95</sup> The only exception is the relative stability between the low dense solid phases, which is not significantly affected.
- By comparing the results of classical simulations of the TIP4P/2005 model with PI simulations of the TIP4PQ/2005 model for the hydrate structures, it has been shown that classical simulations are capable of describing correctly the density of the hydrates for temperatures above 150 K. Furthermore, the relative stability between ice  $I_h$  and hydrates is well described by classical simulations. However, classical simulations cannot describe correctly the densities of the hydrates for temperatures below 150 K. For the structure the classical simulations provide a qualitatively correct description, although to estimate accurately the height of the first peaks of the correlation functions, the quantum treatment is needed. Neither do the classical simulations correctly predict the sublimation enthalpy nor the heat capacity.
- The importance of nuclear quantum effects on the solid phases of water can be rationalized by grouping the ices into three families. The first family is formed by the low dense solid structures ( $I_h$ , sI, sII, and sH), the second family by ices III, V, and VI, and the last family formed by ice II. Phase transitions between ices of the same family are not much affected by nuclear quantum effects (i.e., the importance of nuclear quantum effects is similar for the ices of the same family). The importance of nuclear quantum effects (which increase the energy of a certain solid structure) decreases when moving from the first family to the last. The consequence is that when including quantum effects, the region covered by ice  $I_h$  on the phase diagram (in the  $p$ - $T$  plane) decreases, and the territory left is taken by ices II and III (i.e., lower pressures for the  $I_h$ -II and  $I_h$ -III transitions). Also ice II will increase its presence in the phase diagram (in the  $p$ - $T$  plane) taking regions previously covered by

ices (III, V, and VI), and this is reflected in the higher II-V and II-VI transition pressures in the quantum system.

Returning to the issue of quantum effects on hydrates, it should be mentioned that common guest molecules such as methane or carbon dioxide essentially have classical behavior at the melting temperature of ice; it is expected that any nuclear quantum contributions in hydrates will arise mostly from water. Since the guest molecules can be described reasonably well using classical mechanics, one may expect that the magnitude of the nuclear quantum effects in the gas hydrate is smaller than in the empty hydrate (not by a large amount since hydrates contain approximately one guest molecule for each six water molecules). This may explain the higher values of the thermal expansivity of the gas hydrate with respect to both the empty hydrate and ice  $I_h$ .<sup>9</sup> In that respect the results presented in this work represent an upper limit for the magnitude of the nuclear quantum effects; the addition of the guest molecule would make the system somewhat more classical.

The impact of nuclear quantum effects on the fluid-solid equilibria of hydrates has not been considered in this work, and it would be of interest to study this issue in the future. Preliminary calculations indicate that the melting point for ice  $I_h$  of TIP4PQ/2005 is just 7 K above that of TIP4P/2005. Thus an effective classical potential can reproduce reasonably well the melting point of a quantum model. This strongly suggests that phase equilibria calculations of hydrates can be modeled by classical simulations<sup>96</sup> provided that an effective potential (including implicitly quantum effects through the potential parameters) is used.

## ACKNOWLEDGMENTS

This work has been funded by the DGI (Spain) under Grant Nos. FIS2007-66079-C02-01 and FIS2006-12117-C04-03, the Comunidad Autonoma de Madrid under Grant No. P2009/ESP-1691, and the Universidad Complutense de Madrid under Grant No. 910570. M.M.C. would like to thank University Complutense for the award of a Ph.D. studentship.

<sup>1</sup>E. D. Sloan and C. A. Koh, *Clathrate Hydrates of Natural Gases*, 3rd ed. (CRC, Boca Raton, 2007).

<sup>2</sup>V. F. Petrenko and R. W. Whitworth, *Physics of Ice* (Oxford University Press, Oxford, 1999).

<sup>3</sup>R. McMullan and G. Jeffrey, *J. Chem. Phys.* **42**, 2725 (1965).

<sup>4</sup>C. Mak and R. McMullan, *J. Chem. Phys.* **42**, 2732 (1965).

<sup>5</sup>J. Ripmeester, J. Tse, C. Ratcliffe, and B. Powell, *Nature (London)* **325**, 135 (1987).

<sup>6</sup>H. Docherty, A. Galindo, C. Vega, and E. Sanz, *J. Chem. Phys.* **125**, 074510 (2006).

<sup>7</sup>R. Susilo, S. Alavi, I. L. Moudrakovski, P. Englezos, and J. A. Ripmeester, *ChemPhysChem* **10**, 824 (2009).

<sup>8</sup>S. Alavi, R. Susilo, and J. A. Ripmeester, *J. Chem. Phys.* **130**, 174501 (2009).

<sup>9</sup>H. Tanaka, Y. Tamai, and K. Koga, *J. Phys. Chem. B* **101**, 6560 (1997).

<sup>10</sup>L. J. Florusse, C. J. Peters, J. Schoonman, K. C. Hester, C. A. Koh, S. F. Dec, K. N. Marsh, and E. D. Sloan, *Science* **306**, 469 (2004).

<sup>11</sup>E. D. Sloan, *Nature (London)* **426**, 353 (2003).

<sup>12</sup>J. F. Zhang, R. W. Hawtin, Y. Yang, E. Nakagawa, M. Rivero, S. K. Choi, and P. M. Rodger, *J. Phys. Chem. B* **112**, 10608 (2008).

<sup>13</sup>C. Moon, P. C. Taylor, and P. M. Rodger, *Can. J. Phys.* **81**, 451 (2003).

- <sup>14</sup> C. Moon, R. W. Hawtin, and P. M. Rodger, *Faraday Discuss.* **136**, 367 (2007).
- <sup>15</sup> H. Jiang, K. D. Jordan, and C. E. Taylor, *J. Phys. Chem. B* **111**, 6486 (2007).
- <sup>16</sup> H. Jiang, E. M. Myshakin, K. D. Jordan, and R. P. Warzinski, *J. Phys. Chem. B* **112**, 10207 (2008).
- <sup>17</sup> N. J. English, J. S. Tse, and D. J. Carey, *Phys. Rev. B* **80**, 134306 (2009).
- <sup>18</sup> M. M. Conde, C. Vega, G. A. Tribello, and B. Slater, *J. Chem. Phys.* **131**, 034510 (2009).
- <sup>19</sup> L. C. Jacobson, W. Hujo, and V. Molinero, *J. Phys. Chem. B* **113**, 10298 (2009).
- <sup>20</sup> V. Molinero and E. B. Moore, *J. Phys. Chem. B* **113**, 4008 (2009).
- <sup>21</sup> G. A. Tribello and B. Slater, *J. Chem. Phys.* **131**, 024703 (2009).
- <sup>22</sup> C. McBride, C. Vega, E. Sanz, L. G. MacDowell, and J. L. F. Abascal, *Mol. Phys.* **103**, 1 (2005).
- <sup>23</sup> C. Wei and Z. Hong-Yu, *Chin. Phys. Lett.* **19**, 609 (2002).
- <sup>24</sup> J. H. van der Waals and J. C. Platteeuw, *Adv. Chem. Phys.* **2**, 1 (1959).
- <sup>25</sup> C. McBride, C. Vega, E. G. Noya, R. Ramírez, and L. M. Sesé, *J. Chem. Phys.* **131**, 024506 (2009).
- <sup>26</sup> E. G. Noya, C. Vega, L. M. Sesé, and R. Ramírez, *J. Chem. Phys.* **131**, 124518 (2009).
- <sup>27</sup> J. A. Morrone and R. Car, *Phys. Rev. Lett.* **101**, 017801 (2008).
- <sup>28</sup> F. Paesani and G. A. Voth, *J. Phys. Chem. B* **113**, 5702 (2009).
- <sup>29</sup> R. A. Kuharski and P. J. Rossky, *Chem. Phys. Lett.* **103**, 357 (1984).
- <sup>30</sup> H. A. Stern and B. J. Berne, *J. Chem. Phys.* **115**, 7622 (2001).
- <sup>31</sup> L. Hernández de la Peña, M. S. G. Razul, and P. G. Kusalik, *J. Chem. Phys.* **123**, 144506 (2005).
- <sup>32</sup> C. Vega, M. M. Conde, C. McBride, J. L. F. Abascal, E. G. Noya, R. Ramírez, and L. M. Sesé, *J. Chem. Phys.* **132**, 046101 (2010).
- <sup>33</sup> L. M. Sesé, *J. Chem. Phys.* **126**, 164508 (2007).
- <sup>34</sup> R. Ramírez, C. P. Herrero, A. Antonelli, and E. R. Hernández, *J. Chem. Phys.* **129**, 064110 (2008).
- <sup>35</sup> B. Guillot, *J. Mol. Liq.* **101**, 219 (2002).
- <sup>36</sup> J. L. Finney, *Philos. Trans. R. Soc. London, Ser. B* **359**, 1145 (2004).
- <sup>37</sup> C. Vega, J. Abascal, E. Sanz, L. MacDowell, and C. McBride, *J. Phys.: Condens. Mat.* **17**, S3283 (2005).
- <sup>38</sup> C. Vega, J. L. F. Abascal, and I. Nezbeda, *J. Chem. Phys.* **125**, 034503 (2006).
- <sup>39</sup> J. L. F. Abascal and C. Vega, *J. Chem. Phys.* **123**, 234505 (2005).
- <sup>40</sup> E. Sanz, C. Vega, J. L. F. Abascal, and L. G. MacDowell, *Phys. Rev. Lett.* **92**, 255701 (2004).
- <sup>41</sup> E. Sanz, C. Vega, J. L. F. Abascal, and L. G. MacDowell, *J. Chem. Phys.* **121**, 1165 (2004).
- <sup>42</sup> C. Vega, E. Sanz, and J. L. F. Abascal, *J. Chem. Phys.* **122**, 114507 (2005).
- <sup>43</sup> C. Vega, C. McBride, E. Sanz, and J. L. F. Abascal, *Phys. Chem. Chem. Phys.* **7**, 1450 (2005).
- <sup>44</sup> R. García Fernández, J. L. F. Abascal, and C. Vega, *J. Chem. Phys.* **124**, 144506 (2006).
- <sup>45</sup> C. Vega, M. Martín-Conde, and A. Patrykiewicz, *Mol. Phys.* **104**, 3583 (2006).
- <sup>46</sup> M. M. Conde, C. Vega, and A. Patrykiewicz, *J. Chem. Phys.* **129**, 014702 (2008).
- <sup>47</sup> C. Vega, J. L. F. Abascal, M. M. Conde, and J. L. Aragonés, *Faraday Discuss.* **141**, 251 (2009).
- <sup>48</sup> M. Martín-Conde, L. G. MacDowell, and C. Vega, *J. Chem. Phys.* **125**, 116101 (2006).
- <sup>49</sup> S. Habershon, T. E. Markland, and D. E. Manolopoulos, *J. Chem. Phys.* **131**, 024501 (2009).
- <sup>50</sup> D. Marx and M. H. Müser, *J. Phys.: Condens. Mat.* **11**, R117 (1999).
- <sup>51</sup> M. H. Muser and B. J. Berne, *Phys. Rev. Lett.* **77**, 2638 (1996).
- <sup>52</sup> R. P. Feynman and A. R. Hibbs, *Path-Integrals and Quantum Mechanics* (McGraw-Hill, New York, 1965).
- <sup>53</sup> D. Chandler and P. G. Wolynes, *J. Chem. Phys.* **74**, 4078 (1981).
- <sup>54</sup> M. J. Gillan, in *Computer Modelling of Fluids Polymers and Solids*, NATO ASI Series C, Vol. 293, edited by C. R. A. Catlow, C. S. Parker, and M. P. Allen (Kluwer, Dordrecht, 1990), pp. 155–188.
- <sup>55</sup> D. M. Ceperley, *Rev. Mod. Phys.* **67**, 279 (1995).
- <sup>56</sup> M. P. Allen and D. J. Tildesley, *Computer Simulation of Liquids* (Oxford University Press, Oxford, 1987).
- <sup>57</sup> J. Lobaugh and G. A. Voth, *J. Chem. Phys.* **106**, 2400 (1997).
- <sup>58</sup> W. Shinoda and M. Shiga, *Phys. Rev. E* **71**, 041204 (2005).
- <sup>59</sup> M. W. Mahoney and W. L. Jorgensen, *J. Chem. Phys.* **115**, 10758 (2001).
- <sup>60</sup> L. Hernández de la Peña and P. G. Kusalik, *J. Chem. Phys.* **121**, 5992 (2004).
- <sup>61</sup> G. S. Fanourgakis, G. K. Schenter, and S. S. Xantheas, *J. Chem. Phys.* **125**, 141102 (2006).
- <sup>62</sup> S. Habershon, G. S. Fanourgakis, and D. E. Manolopoulos, *J. Chem. Phys.* **129**, 074501 (2008).
- <sup>63</sup> G. S. Fanourgakis, T. E. Markland, and D. E. Manolopoulos, *J. Chem. Phys.* **131**, 094102 (2009).
- <sup>64</sup> M. Yousuf, S. Qadri, D. Knies, K. Grabowski, R. Coffin, and J. Pohlman, *Appl. Phys. A: Mater. Sci. Process.* **78**, 925 (2004).
- <sup>65</sup> L. Pauling, *The Nature of the Chemical Bond and the Structure of Molecules and Crystals: An Introduction to Modern Structural Chemistry* (Cornell University Press, Ithaca, NY, 1960).
- <sup>66</sup> F. Hollander and G. A. Jeffrey, *J. Chem. Phys.* **66**, 4699 (1977).
- <sup>67</sup> S. W. Peterson and H. A. Levy, *Acta Crystallogr.* **1957**, 72 (1957).
- <sup>68</sup> S. W. Rick and D. L. Freeman, *J. Chem. Phys.* **132**, 054509 (2010).
- <sup>69</sup> V. Buch, P. Sandler, and J. Sadlej, *J. Phys. Chem. B* **102**, 8641 (1998).
- <sup>70</sup> J. D. Bernal and R. H. Fowler, *J. Chem. Phys.* **1**, 515 (1933).
- <sup>71</sup> M. Parrinello and A. Rahman, *J. Appl. Phys.* **52**, 7182 (1981).
- <sup>72</sup> S. Yashonath and C. N. R. Rao, *Mol. Phys.* **54**, 245 (1985).
- <sup>73</sup> D. Frenkel and B. Smit, *Understanding Molecular Simulation* (Academic, London, 1996).
- <sup>74</sup> A. G. Ogienko, A. V. Kurnosov, A. Y. Manakov, E. G. Larionov, A. I. Ancharov, M. A. Sheromov, and A. N. Nesterov, *J. Phys. Chem. B* **110**, 2840 (2006).
- <sup>75</sup> S. Takeya, M. Kida, H. Minami, H. Sakagami, A. Hachikubo, N. Takahashi, H. Shoji, V. Soloviev, K. Wallmann, N. Biebow, A. Obzhirov, A. Salomatin, and J. Poort, *Chem. Eng. Sci.* **61**, 2670 (2006).
- <sup>76</sup> P. M. Rodger, *J. Phys. Chem.* **94**, 6080 (1990).
- <sup>77</sup> C. Bourry, J. Charlou, J. Donval, M. Brunelli, C. Focsa, and B. Chazallon, *Geophys. Res. Lett.* **34**, L22303 (2007).
- <sup>78</sup> D. W. Davidson, Y. P. Handa, C. I. Ratcliffe, J. A. Ripmeester, J. S. Tse, J. R. Dahn, F. Lee, and L. D. Calvert, *Mol. Cryst. Liq. Cryst.* **141**, 141 (1986).
- <sup>79</sup> R. Feistel and W. Wagner, *J. Phys. Chem. Ref. Data* **35**, 1021 (2006).
- <sup>80</sup> P. W. Bridgman, *Proc. Am. Acad. Arts Sci.* **47**, 441 (1912).
- <sup>81</sup> E. Whalley, *J. Chem. Phys.* **81**, 4087 (1984).
- <sup>82</sup> H. B. Callen, *Thermodynamics and an Introduction to Thermostatistics* (Wiley, New York, 1985).
- <sup>83</sup> B. Guillot and Y. Guissani, *Mol. Phys.* **87**, 37 (1996).
- <sup>84</sup> L. M. Sesé, *Mol. Phys.* **85**, 931 (1995).
- <sup>85</sup> J. L. Aragonés, E. G. Noya, J. L. F. Abascal, and C. Vega, *J. Chem. Phys.* **127**, 154518 (2007).
- <sup>86</sup> See supplementary material at <http://dx.doi.org/10.1063/1.3353953> for values of the enthalpies for ices I<sub>h</sub>, II, III, V, VI, sI, sII, and sH at 1 bar for the six temperatures considered in this work.
- <sup>87</sup> H. J. C. Berendsen, J. R. Grigera, and T. P. Straatsma, *J. Phys. Chem.* **91**, 6269 (1987).
- <sup>88</sup> Y. Koyama, H. Tanaka, and K. Koga, *J. Chem. Phys.* **122**, 074503 (2005).
- <sup>89</sup> D. W. Davidson, *Clathrate Hydrates in Water: A Comprehensive Treatise* (Butterworths, Boston, MA, 1983).
- <sup>90</sup> O. S. Subbotin, T. Ikeshiji, V. R. Belosludov, J. Kudoh, R. V. Belosludov, and Y. Kawazoe, *J. Phys.: Conf. Ser.* **29**, 206 (2006).
- <sup>91</sup> A. V. Kurnosov, A. Y. Manakov, V. Y. Komarov, V. I. Voronin, A. E. Teplikh, and Y. A. Dyadin, *Dokl. Phys. Chem.* **381**, 303 (2001).
- <sup>92</sup> See: <http://www.lsbu.ac.uk/water/>.
- <sup>93</sup> G. S. Fanourgakis and S. S. Xantheas, *J. Chem. Phys.* **128**, 074506 (2008).
- <sup>94</sup> K. Szalewicz, C. Leforestier, and A. van der Avoird, *Chem. Phys. Lett.* **482**, 1 (2009).
- <sup>95</sup> R. Kumar and J. L. Skinner, *J. Phys. Chem. B* **112**, 8311 (2008).
- <sup>96</sup> M. R. Walsh, C. A. Koh, E. D. Sloan, A. K. Sum, and D. T. Wu, *Science* **326**, 1095 (2009).